Virchows Archiv (2024) 484:103–117
https://doi.org/10.1007/s00428-023-03697-1

ORIGINAL ARTICLE

Branchioma: immunohistochemical and molecular genetic study of 23 cases highlighting frequent loss of retinoblastoma 1 immunoexpression

Martina Bradová[1,2] · Lester D. R. Thompson[3] · Martin Hyrcza[4] · Tomáš Vaněček[5] · Petr Grossman[5] · Michael Michal Jr.[1,2] · Veronika Hájková[5] · Touraj Taheri[6] · Niels Rupp[7,8] · David Suster[9] · Sunil Lakhani[10] · Dimitar Hadži Nikolov[11] · Radim Žalud[11] · Alena Skálová[1,2] · Michal Michal[1,2] · Abbas Agaimy[12]

Received: 28 September 2023 / Revised: 25 October 2023 / Accepted: 3 November 2023 / Published online: 14 November 2023

Abstract

Branchioma is an uncommon benign neoplasm with an adult male predominance, typically occurring in the lower neck region. Different names have been used for this entity in the past (ectopic hamartomatous thymoma, branchial anlage mixed tumor, thymic anlage tumor, biphenotypic branchioma), but currently, the term branchioma has been widely accepted. Branchioma is composed of endodermal and mesodermal lineage derivatives, in particular epithelial islands, spindle cells, and mature adipose tissue without preexistent thymic tissue or evidence of thymic differentiation. Twenty-three branchiomas were evaluated morphologically. Eighteen cases with sufficient tissue were assessed by immunohistochemistry, next-generation sequencing (NGS) using the Illumina Oncology TS500 panel, and fluorescence in situ hybridization (FISH) using an RB1 dual-color probe. All cases showed a biphasic morphology of epithelial and spindle cells with intermingled fatty tissue. Carcinoma arising in branchioma was detected in three cases. The neoplastic cells showed strong AE1/3 immunolabeling (100%), while the spindle cells expressed CD34, p63, and SMA (100%); AR was detected in 40–100% of nuclei (mean, 47%) in 14 cases. Rb1 showed nuclear loss in ≥ 95% of neoplastic cells in 16 cases (89%), while two cases revealed retained expression in 10–20% of tumor cell nuclei. NGS revealed a variable spectrum of likely pathogenic variants ($n=5$) or variants of unknown clinical significance ($n=6$). Loss of Rb1 was detected by FISH in two cases. Recent developments support branchioma as a true neoplasm, most likely derived from the rudimental embryological structures of endoderm and mesoderm. Frequent Rb1 loss by immunohistochemistry and heterozygous deletion by FISH is a real pitfall and potential confusion with other Rb1-deficient head and neck neoplasms (i.e., spindle cell lipoma), especially in small biopsy specimens.

Keywords Branchioma · Ectopic hamartomatous thymoma · Head · And neck · Retinoblastoma 1 · RET · CD34

✉ Martina Bradová
bradova@biopticka.cz

[1] Department of Pathology, Faculty of Medicine in Pilsen, Charles University, E. Benese 13, 305 99 Pilsen, Czech Republic

[2] Bioptic Laboratory, Ltd, Pilsen, Czech Republic

[3] Head and Neck Pathology Consultations, Woodland Hills, CA, USA

[4] Department of Pathology and Laboratory Medicine, University of Calgary, Calgary Laboratory Services, Foothills Medical Centre, Calgary, AB, Canada

[5] Molecular and Genetic Laboratory, Bioptic Laboratory, Ltd, Pilsen, Czech Republic

[6] School of Medicine and Pathology Queensland, University of Queensland, Brisbane, Australia

[7] Department of Pathology and Molecular Pathology, University Hospital Zurich, Zurich, Switzerland

[8] Faculty of Medicine, University of Zurich, Zurich, Switzerland

[9] Department of Pathology, Rutgers University New Jersey Medical School, Newark, NJ, USA

[10] School of Medicine and Pathology Queensland, University of Queensland, UQCCR, Herston, Australia

[11] Pathology Department, Regional Hospital Kolin, JSC, Kolin, Czech Republic

[12] Institute of Pathology, University Hospital Erlangen, Friedrich-Alexander University Erlangen-Nürnberg (FAU), Comprehensive Cancer Center (CCC) Erlangen-EMN, Erlangen, Germany

Introduction

Branchiomas are rare benign lower neck tumors with an adult male predominance [1]. In the past, the tumor received several names trying to reflect its most likely histogenetic origin, in particular thymic anlage tumor, branchial anlage mixed tumor, or ectopic hamartomatous thymoma. However, it became evident that none of these names really describes the true nature of this lesion. In order to avoid taxonomic confusion, a descriptive term reflecting the entodermal and mesodermal origin of the tumor was introduced as a common basis for tumors arising from or recapitulating the branchial apparatus. The English literature contains 87 cases of this entity with four cases showing a concurrent malignant histology [2–7].

Branchioma (biphenotypic branchioma) is composed of an admixture of adipocytic tissue, spindled cells, and epithelial nests, the latter potentially arranged in different architectural [8]. Epithelial and spindle cells are immunoreactive for pancytokeratins, p63 and p40, but only spindle cells are positive for smooth muscle actin and CD34 [9, 10]. The last components represent delicate spindly cells, usually irregularly interspersed between the previous components, which are negative for cytokeratins and positive for CD34. The frequent expression of AR by the tumor cells has been linked to the male predominance of branchiomas [11]. In a recent case report, we published a case of branchioma with neuroendocrine-like tumor morphology showing immunohistochemical loss of Rb1 expression, while FISH showed no alteration in the *Rb1* gene [8].

This study specifically aimed to establish the presence of Rb1 alterations in a series of branchiomas, especially set within the context of the differential with spindle cell lipoma and spindle cell predominant trichodiscoma (https://www.illumina.com/content/dam/illumina-marketing/documents/products/gene_lists/gene_list_trusight_oncology_500.xlsx.) [12–14].

Materials and methods

Histology and immunohistochemistry

For conventional microscopy, tissues were fixed in formalin, routinely processed, embedded in paraffin (FFPE), cut, and stained with hematoxylin and eosin.

For immunohistochemistry, 4-µm-thick sections were cut from paraffin blocks and mounted on positively charged slides (TOMO, Matsunami Glass IND, Osaka, Japan). Sections were processed on a BenchMark ULTRA (Ventana Medical Systems, Tucson, AZ), deparaffinized, and subjected to heat-induced epitope retrieval by immersion in a CC1 solution (pH 8.6) at 95 °C. The primary antibodies used in this study are summarized in Table 1. Visualization was performed using the ultraView Universal DAB Detection Kit (Roche, Tucson, AZ) and ultraView Universal Alkaline Phosphatase Red Detection Kit (Roche, Tucson, AZ). The slides were counterstained with Mayer's hematoxylin. Appropriate positive controls were employed.

Molecular genetic study

Archer FusionPlex assay

The in-house customized version of Archer FusionPlex Sarcoma kit was used to construct a cDNA library for detecting fusion transcripts and point mutations in 88

Table 1 Antibodies used for the immunohistochemical study

Antibody	Clone	Dilution	Antigen retrieval/time	Source
CD34	QBEnd/10	1:200	CC1/64 min	DAKO Cytomation
AE1/AE3	AE1/AE3	RTU	EnVision high pH/30 min	DAKO
OSCAR	IsoType:IgG2a	1:500	EnVision high pH/30 min	Covance
p63	DAK-p63	RTU	EnVision low pH/30 min	DAKO
SOX10	SP267	RTU	CC1/64 min	Cell Marque
S-100 protein	Polyclonal	RTU	EnVision high pH/30 min	DAKO
Smooth muscle actin	1A4	RTU	CC1/36 min	Cell Marque
Androgen receptor	SP107	RTU	CC1/64 min	Cell Marque
Retinoblastoma 1	G3-245	1:25	CC1/66 min	BD Biosciences
Ki-67	MIB-1	RTU	EnVision high pH/30 min	DAKO

RTU ready to use
CC1 — EDTA buffer, pH 8.6, 95 °C
EnVision high pH, pH 9.0, 97 °C
EnVision low pH, pH 6.0, 97 °C
min, minutes

Table 2 Clinical data and follow-up

No	Age/sex	Site	Size (mm)	Therapy	Symptoms	Diagnosis (original diagnosis)	Follow-up (months)	Previously published — citation number or PMID
1	78/M	Left supraclavicular area	60	Complete excision	Neck mass	Branchioma (metastasis of neuroendocrine tumor)	8 ANED	No. 8
2	43/M	Suprasternal area	38	Complete excision	120 months with growing mass	Branchioma	60 ANED	
3	65/M	Supraclavicular area	42	Complete excision	4 months with growing mass	Branchioma	12 ANED	
4	39/M	Supraclavicular area	40	Complete excision		Carcinoma ex branchioma	3 ANED	No. 2 — case 2 No. 3 — case 2
5	38/M	Suprasternal area	30	Complete excision		Branchioma	6 ANED	No. 3 — case 3
6	36/M	Suprasternal area	15	Complete excision	24 months with growing mass	Branchioma with myoid differentiation	6 ANED	No. 3 — case 4
7	43/M	Suprasternal area	30	Complete excision		Branchioma with clear cells differentiation	NA	No. 17
8	?/M	Suprasternal area	NA	Complete excision		Branchioma with syringomatoid ducts	NA	
9	56/M	Supraclavicular area	NA	Complete excision		Branchioma	NA	
10	52/M	Supraclavicular area	15	Complete excision	3 months with growing mass	Branchioma	8 ANED	PMID: 12390415
11	71/F	Interface of the posterior axillary region and back	35	Complete excision	360 months with growing mass	Branchioma	143 DOUR	PMID: 15279645
12	70/M	Neck area	22	Complete excision		Branchioma (neurofibroma)	NA	
13	31/M	Right supraclavicular area	60	Complete excision	6 months with growing mass	Carcinoma ex branchioma	60 ANED	No. 2 — case 1 No. 3 — case 1 No. 4
14	80/M	Suprasternal area	10	Complete excision	2 months with growing mass	Branchioma (fibroma)	NA	
15	56/M	Chest midline area	41	Complete excision	NA	Branchioma	24 ANED	
16	55/M	Left supraclavicular area	50	Complete excision	NA	Branchioma (biphasic synovial sarcoma)	0	
17	41/M	Supraclavicular area	25	Complete excision	NA	Branchioma (biphasic synovial sarcoma)	0	
18	51/M	Left supraclavicular area	18	Complete excision	18 months with growing mass	Branchioma (basal cell adenoma)	20 ANED	
19	70/F	Suprasternal area	35	Excision with positive margin	12 months with growing mass	Intraductal carcinoma ex branchioma (salivary duct carcinoma)	48 ANED	No. 5 — case 2 No. 6 — case 3
20	50/M	Suprasternal area	44	Complete excision	48 months with growing mass	Branchioma (myoepithelioma)	72 ANED	No. 6 — case 1

Table 2 (continued)

No	Age/sex	Site	Size (mm)	Therapy	Symptoms	Diagnosis (original diagnosis)	Follow-up (months)	Previously published — citation number or PMID
21	37/M	Right supraclavicular area	53	Complete excision	Cyst-like lesion	Branchioma	LOF	
22	NA/M	Supraclavicular area	30	Excision	Suspicious enlarged lymph node	Branchioma	LOF	
23	55/M	Anterior chest wall	80	Complete excision	Slowly growing, nonpainful mass	Branchioma	60 ANED	

M male, *F* female, *ANED* alive not evidence of disease, *DOUR* died of unrelated reasons, *LOF* lost to follow-up, *NA* not available

Table 3 Clinicopathological and histological data of all carcinomas ex branchioma reported in the English literature (three cases included in the recent study)

No	Age/sex	Site	Size (mm)	Therapy	Pattern of the carcinoma	IHC profile AR/S100	Molecular findings	Follow-up (months)
1*	39/M	Supraclavicular area	40	Complete excision	Intraductal carcinoma of apocrine type	Positive/negative	NA	3 ANED
2**	31/M	Right supraclavicular area	60	Complete excision	Intraductal carcinoma with cribriform morphology	Negative/negative	NA	60 ANED
3***	70/F	Suprasternal area	35	Excision with positive margin	Intraductal carcinoma of apocrine type	Positive/negative	*HRAS* c.181C > A p.(Gln61Lys) AF: 29% *PIK3CA* c.1624G > A p.(Glu542Lys) AF: 8% *CHD2* c.4173dup p.(Gln1392ThrfsTer17) AF: 7% *SLIT2* c.162_163dup p.(Arg55ProfsTer9) AF: 40%*	48 ANED
4+	62/M	Right supraclavicular area	75	Resection	Adenocarcinoma NOS with low-grade (tubular, cord, and solid) and high-grade (tubular, cribriform, and solid) areas	Positive/negative	*KRAS* p.(Q61H) AF: 52.4% *TP53* p.(R175H) AF: 39.7%	36 ANED

ANED alive not evidence of disease, *AR* androgen receptors, *F* female, *M* male

*Recent case no. 4 and previously published: citation no. 2 — case 2, citation no. 3 — case 2

**Recent case no. 13 and previously published: citation no. 2 — case 1; citation no. 3 — case 1; citation no. 4

***Recent case no. 19 and previously published: citation no. 5 — case 2; citation no. 6 — case 3

+Previously published: citation no. 7

and 14 genes, respectively. The complete list of genes and mutations covered by this assay has been reported previously [12]. All steps were performed according to the manufacturer's instructions, and the library was sequenced on an Illumina platform as described previously [13].

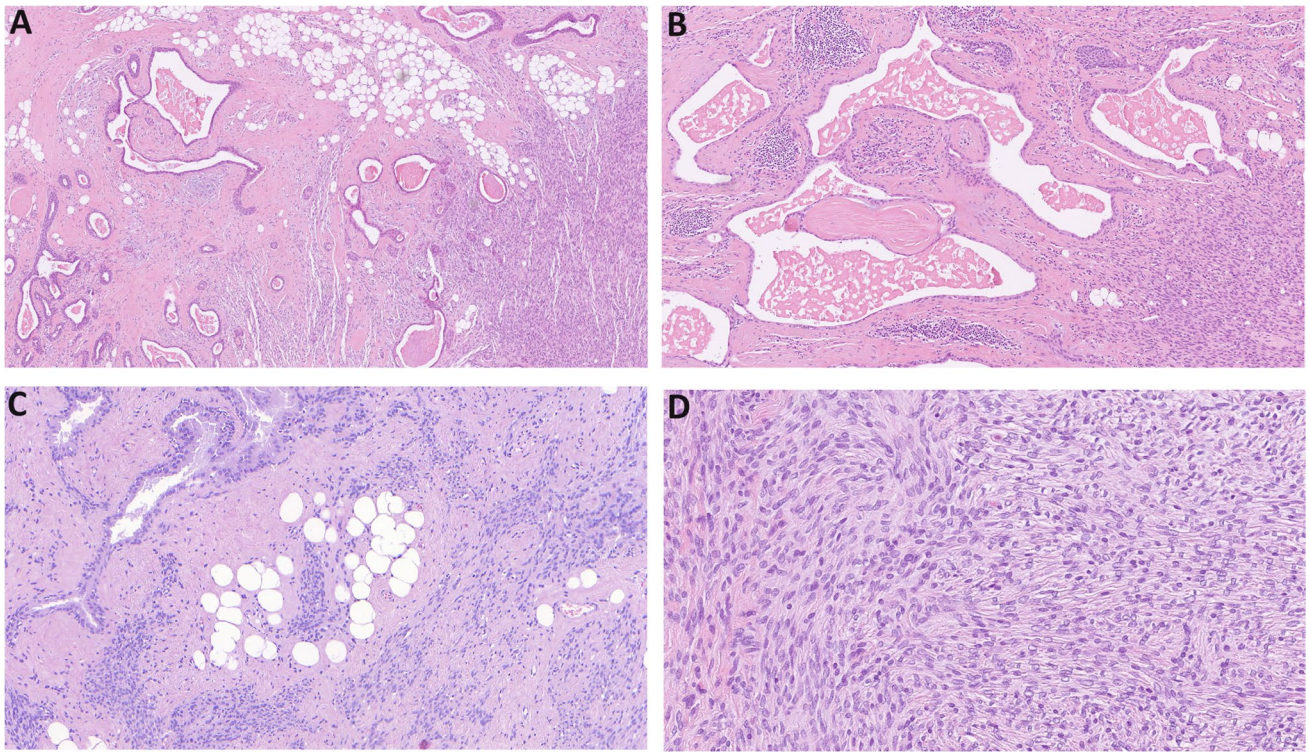

Fig. 1 A classic branchioma composed of a combination of epithelial component, cystic structures, and solid epithelial nests with intermingled fatty tissue (**A**) and spindle cells (**B**). Plump epithelioid to spindle cells are arranged in haphazard (**C**), storiform, or fascicular fashion, resembling monophasic synovial sarcoma (**D**)

Illumina TruSight Oncology 500 assay

The cases were analyzed using the commercially available TruSight Oncology 500 assay from Illumina. This panel can analyze both DNA and RNA. The DNA analysis interrogates 523 genes for single nucleotide variants and indels, and the RNA analysis interrogates 55 genes. The complete list of genes can be found on manufacturer's website (https://www.illumina.com/content/dam/illumina-marketing/documents/products/gene_lists/gene_list_trusight_oncology_500.xlsx).

Briefly, DNA libraries were prepared using the TruSight Oncology 500 Kit (Illumina) according to the manufacturer's protocol, except for DNA enzymatic fragmentation which was done using KAPA FragKit (KAPA Biosystems, Washington, MA). Sequencing was performed on the NextSeq 550 sequencer (Illumina) following manufacturer's recommendations. Data analysis (DNA variant filtering and annotation) was performed using the Omnomics NGS analysis software (Euformatics, Finland). Custom variant filter was set up including only non-synonymous variants with coding consequences, read depth greater than 50, benign variants according to the ClinVar database were also excluded [14]. The remaining subset of variants was checked visually, and suspected artefactual variants were excluded.

Detection of Rb1 deletion by FISH

For the detection of *Rb1* loss, the probe ZytoLight® SPEC Rb1/13q12 Dual Color Probe (ZytoVision GmbH, Bremerhaven, Germany) was used. The fluorescence in situ hybridization (FISH) procedure was performed as described previously [15].

FISH interpretation

One hundred randomly selected nonoverlapping tumor cell nuclei were evaluated in all analyzed samples. *Rb1* gene loss was recorded as the number of cells with loss divided by the total number of cells counted. The test was interpreted as positive if > 45% of the counted nuclei had gene loss (mean + 3 standard deviations in normal non-neoplastic control tissues).

Results

Demographic and clinical features

The clinicopathological data of the 23 branchioma cases are summarized in Table 2. In addition, cases of

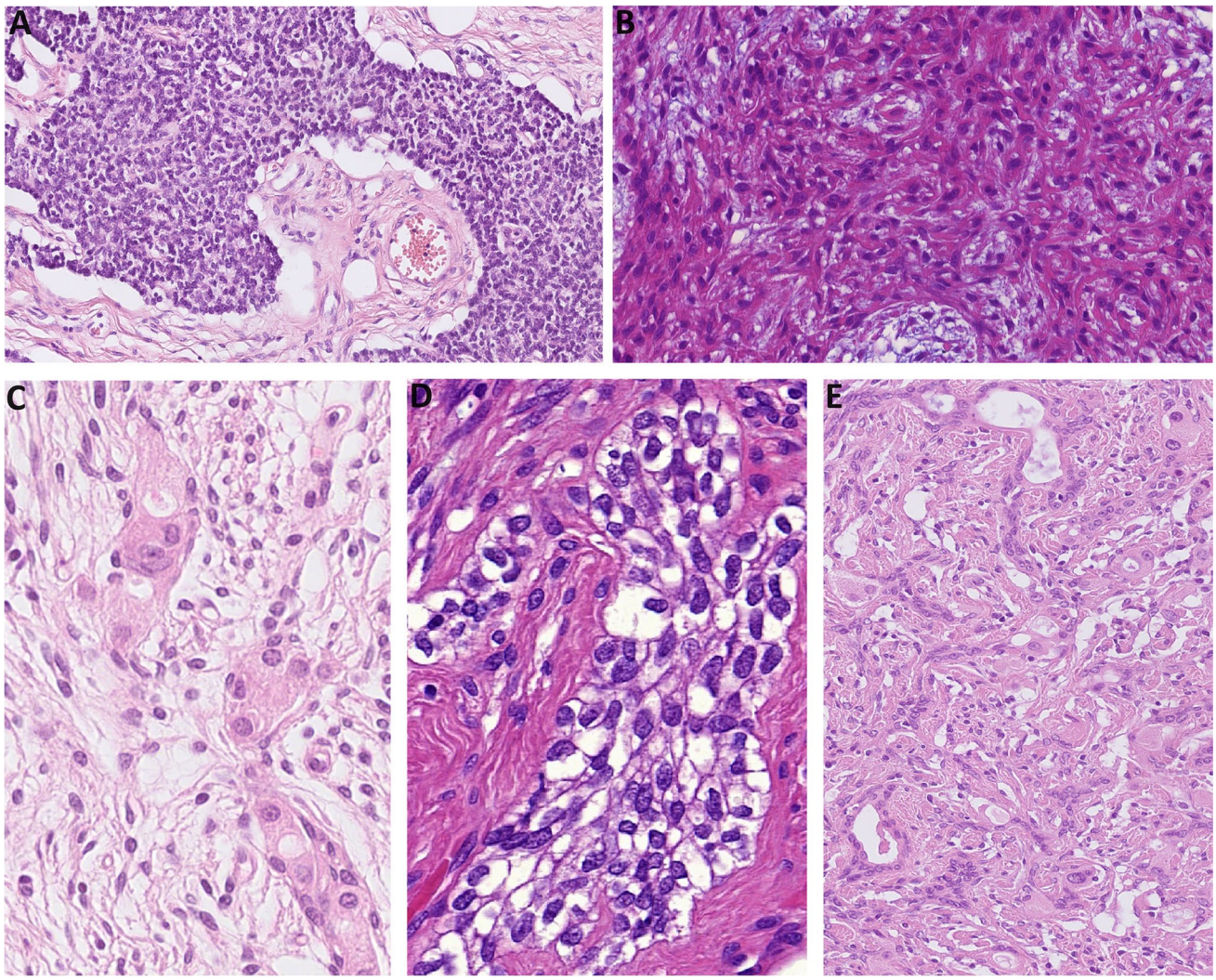

Fig. 2 Case 1 was composed of sheets and cords of neuroendocrine-like epithelial cells with peripheral clefting, with intermingled spindle cells (**A**). Case 5 showed prominent myoid spindle cells without cross striations surrounded by myxoid stroma (**B**). Case 6 showed prominent squamoid cords nestled in a spindle cell background (**C**). Case 7 demonstrated clear cell nests or cords reminiscent of parathyroid gland (**D**). Case 8 had syringomatoid ducts and tumor cells with abundant granular cytoplasm (**E**)

carcinoma ex branchioma are listed in a separate Table 3. There were 21 males and two females aged between 31 and 80 years, with both median and mean age of 52 years. The tumors were localized in the supraclavicular area ($n = 11$), suprasternal area ($n = 8$), chest wall ($n = 2$), neck ($n = 1$), and in one case at the junction of the posterior axillary region and the back. The median tumor size was 35 mm (range 10–80 mm). Fourteen patients complained of slowly enlarging mass lasting from 2 months to 30 years (median 15 months). None of the cases showed signs of recurrance or metastasis. All cases were treated by simple excision without adjuvant therapy including cases with carcinoma.

Fifteen patients were alive without evidence of disease with a median 16 months of follow-up (mean 25.8 months, range 0–72 months), and one patient died of unknown reasons 143 months after surgery. Follow-up data were not available in seven cases.

Histological features

Key histological and immunohistochemical features of the branchioma are summarized in Supplementary file 1. Twenty tumors were well-circumscribed classic branchiomas consisting of an admixture of spindle cells, epithelial cells, and adipose tissue with interspersed bland spindle cells. The epithelial component showed either cystic structures layered by biphasic flattened epithelium or solid

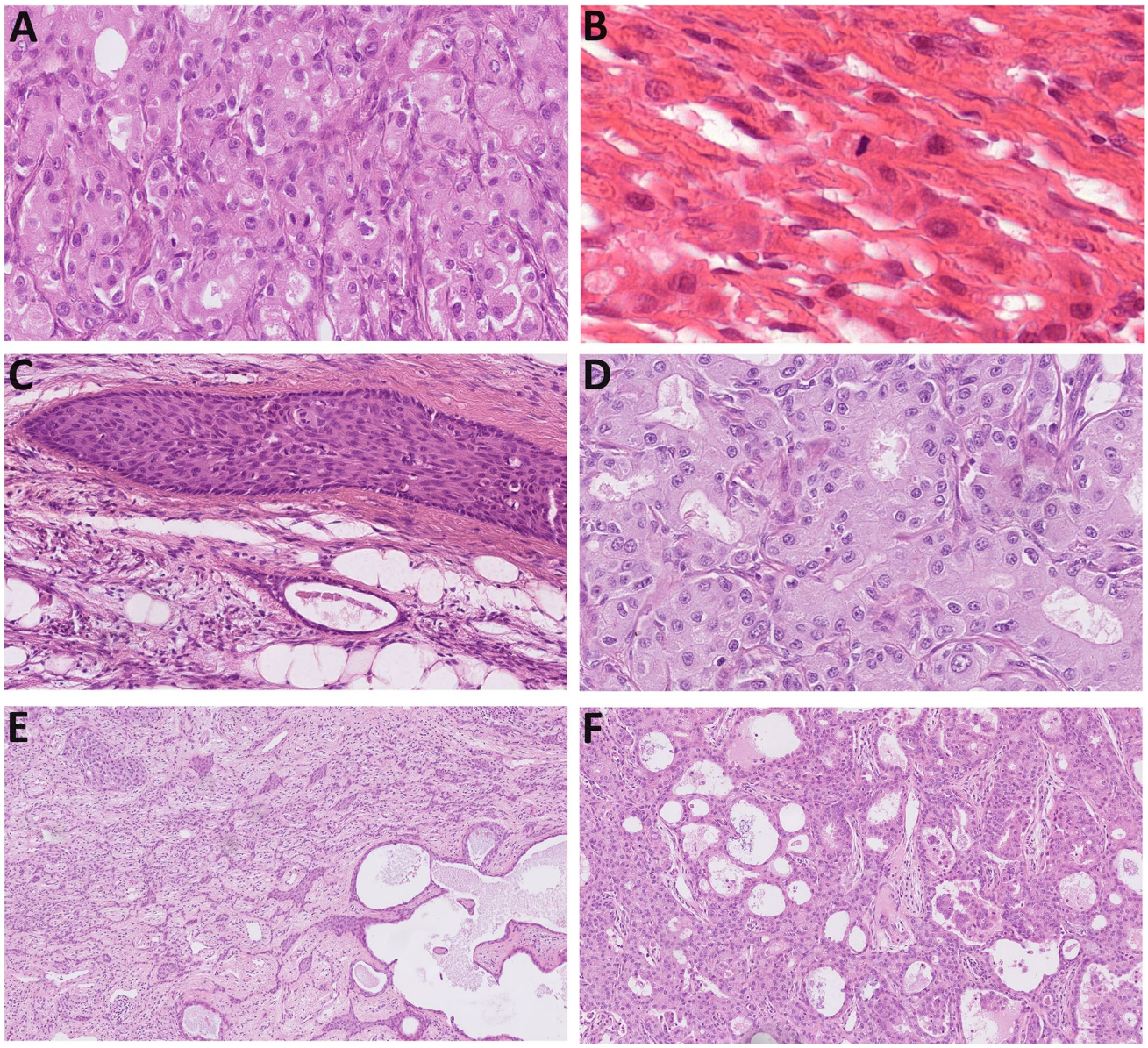

Fig. 3 Case 4 showed an epithelial adenomatoid component arranged in solid sheets, along with cords or glands with a back-to-back appearance similar to ductal breast carcinoma (**A**). Tumor cells had granular cytoplasm; mitoses were unevenly dispersed (**B**). Case 13 had two different epithelial components: one with classic solid to cystic structures with squamous lining resembling syringomatoid ducts and squamoid nests with multiple mitoses (**C**). The second component grew in an adenomatoid cribriform pattern with Roman bridging resembling intraductal carcinoma of breast and salivary gland (**D**). Case 19 demonstrated an epithelial proliferation with cystic changes lined by squamous epithelium (lower right) with a direct transition to solid IC (upper left) (**E**). The IC part was a continuum of typical and atypical ductal hyperplasia growing directly into IC with Roman bridges, and papillary or solid growth (**F**)

nests (Fig. 1A, B). Plump spindle cells were arranged in a haphazard, storiform, or fascicular fashion (Fig. 1C, D).

In case 1, a neuroendocrine tumor-like morphology was observed (previously reported [8]), but the tumor did not express any neuroendocrine markers investigated (synaptophysin, chromogranin, and INSM1) (Fig. 2A). Another previously described case (case 5) showed extensive myoid differentiation, mainly in the myxoid areas. The spindle cells were plump and highly eosinophilic without cross striation. They were immunoreactive for smooth muscle actin, but non-reactive for rhabdomyoblastic markers including desmin, myogenin, and MyoD1 (Fig. 2B) [3]. In case 6, multinucleated giant cells were scattered throughout the tumor together with epithelial formations resembling squamous pearls mimicking the sarcomatoid subtype of squamous cell carcinoma (SCC) (Fig. 2C) [3]. In case 7, clear cells were predominant, the epithelial cells were arranged in clear cell cords reminiscent

Table 4 Immunohistochemical results of 20 cases of branchiomas and three cases of carcinomas ex branchioma

No	Rb1	CD34	AE1/3	SMA	p63	S100	SOX10	AR	MIB1 proliferation index
1	Loss (< 5%)	Biphasic, + in spindle cells	+ in both components	Biphasic, + in spindle cells	Biphasic, + in spindle cells and myoepithelial cells	Fatty tissue only	Neg	40%	5%
2	Loss (< 1%)	Biphasic, + in spindle cells	+ in both components	Biphasic, + in spindle cells	Biphasic, + in spindle cells and myoepithelial cells	Fatty tissue only	Neg	40%	5%
3	Loss (< 1%)	Biphasic, + in spindle cells	+ in both components	Biphasic, + in spindle cells	Biphasic, + in spindle cells and myoepithelial cells	Few cells — fatty tissue +	Neg	40%	3%
4	Loss (in B and IC)	Negative	+ in both components of B and + in IC	Biphasic, + in spindle cells	Biphasic, + in spindle cells and myoepithelial cells	Fatty tissue only	Neg	IC 60%, B 5%	1%
5	Loss	Negative	+ in both components	Biphasic, + in spindle cells but weak	Biphasic, + in spindle cells and myoepithelial cells	Fatty tissue only	Neg	Negative	0%
6	Loss	W and F spindle cells	+ in both components	Biphasic, + in spindle cells	Negative	F + < 7%	Neg	Negative	0%
7	NA	NA	NA	NA	NA	NA	Neg	NA	NA
8	Loss (< 1%)	Biphasic, + in spindle cells	+ in both components	F + in spindle cells and myoepithelial cells	Biphasic, + in spindle cells and myoepithelial cells	Fatty tissue only	Neg	70%	4%
9	NA	NA	NA	NA	NA	NA	NA	NA	NA
10	NA	NA	NA	NA	NA	NA	NA	NA	NA
11	Loss	Biphasic, + in spindle cells	+ in both components	F + in spindle cells and myoepithelial cells	Biphasic, + in spindle cells and myoepithelial cells	Negative	Neg	Negative	2%
12	NA	NA	NA	NA	NA	NA	NA	NA	NA
13	Loss (in B and IC)	F biphasic, + in spindle cells	+ in both components	Biphasic, + in spindle cells	Biphasic, + in spindle cells and myoepithelial cells	Fatty tissue only	Neg	Negative (IC and B)	< 1%
14	Loss	Biphasic, + in spindle cells	+ in both components of B and + in IC	F + in spindle cells and myoepithelial cells	Biphasic, + in spindle cells and myoepithelial cells	Fatty tissue only	Neg	40%	< 5%
15	NA	NA	NA	NA	NA	NA	NA	NA	NA
16	Loss (< 3%)	Biphasic, + in spindle cells	+ in both components	Biphasic, + in spindle cells	Biphasic, + in spindle cells and myoepithelial cells	NA	Neg	75%	
17	Loss (< 1%)	Biphasic, + in spindle cells	+ in both components	Biphasic, + in spindle cells	Biphasic, + in spindle cells and myoepithelial cells	NA	Neg	40%	
18	+ (25%)	Biphasic, + in spindle cells	+ in both components	Biphasic, + in spindle cells	Biphasic, + in spindle cells and myoepithelial cells	Fatty tissue only	Neg	85%	1%

Table 4 (continued)

No	Rb1	CD34	AE1/3	SMA	p63	S100	SOX10	AR	MIB1 proliferation index
19	Loss (< 2%) in IC and loss in B	Biphasic, + in spindle cells	+ in both components of B and + in IC	Biphasic, + in spindle cells	Biphasic, + in spindle cells and myoepithelial cells	Fatty tissue only	Neg	IC 100%, B 5%	20%
20	Loss	Biphasic, + in spindle cells	+ in both components	Biphasic, + in spindle cells	Biphasic, + in spindle cells and myoepithelial cells	Fatty tissue only	Neg	80%	< 1%
21	Loss	Biphasic, + in spindle cells	+ in both components	F + in spindle cells and myoepithelial cells	Biphasic, + in spindle cells and myoepithelial cells	Fatty tissue only	Neg	50%	< 2%
22	Loss (< 5%)	Biphasic, + in spindle cells	+ in both components	Biphasic, + in spindle cells	Biphasic, + in spindle cells and myoepithelial cells	Negative	NA	80%	
23	+ (25%)	Biphasic, + in spindle cells	+ in both components	Biphasic, + in spindle cells	Biphasic, + in spindle cells and myoepithelial cells	Fatty tissue only	Neg	80%	< 5%

AR androgen receptor, *B* branchioma, *F* focal, *IC* intraductal carcinoma, *NA* not available, + positive, *Rb1* retinoblastoma 1

of the structure of the parathyroid gland, but the tumor was negative for parathyroid hormone (Fig. 2D) [16]. Case 8 was composed of spindle cells and epithelioid cells with the appearance of syringomatoid ducts with atypia. A granular cell component was also present (Fig. 2E).

In three cases (3/23, 13%), a carcinoma developed in the background of branchioma (Table 3). All cases were previously reported [2–6]. In case 4, the tumor consisted of all three components typical of branchioma, but the epithelial component was arranged in solid sheets formed by squamous cells, cords, or glands with back-to-back glands mimicking ductal breast carcinoma. The tumor cells had granular cytoplasm and mitoses were unevenly dispersed [2, 3] (Fig. 3A, B). Case 13 was composed of different epithelial structures, one with classic solid to cystic structures with squamous lining resembling syringomatoid ducts and the second with adenomatoid cribriform pattern and Roman bridging resembling intraductal carcinoma (IC) of the salivary gland (Fig. 3C, D). A scanned whole slide image of the case is available at https://pathpresenter.net/public/display?token=66640ea4. The tumor cells showed granular cytoplasm and frequent mitoses, including atypical ones [2–4]. Case 19 showed a developmental continuum of typical and atypical ductal hyperplasia evolving into IC (Fig. 3E, F) [5, 6]. A scanned whole slide image of the case is available at https://pathpresenter.net/public/display?token=c7cc23dd.

Immunohistochemistry

Immunohistochemistry was performed in 18 cases (18/23; 78%) in which tissue blocks were available (all cases without material were classic branchiomas without malignant transformation) and the results are summarized in Table 4.

All 15 cases of typical branchioma showed a classical IHC profile. Both the spindle and epithelial components were AE1/3 (Fig. 4A) and p63 (Fig. 4B) positive. Spindle cells additionally expressed CD34 (Fig. 4C) and SMA. AR was positive in 12/15 tested cases with an average of 60% positive tumor nuclei (range 40–85%) (Fig. 4D). Proliferative activity was low with an average Ki-67 (MIB1) proliferation index of 3% (range 0 to 5%). Rb1 immunostaining was performed in 15 cases, of which six cases were completely negative, seven cases showed < 5% nuclear reactivity, and two cases were positive (maximum of 25% positive tumor cell nuclei) (Fig. 4E).

Three cases of carcinoma ex branchioma were located in the background of branchioma with a typical IHC profile. The carcinoma component showed strong expression of AE1/3 (3/3) (Fig. 5A), while CD34, SMA, SOX10, and S100 protein were negative in the carcinoma component (Fig. 5B, C). The myoepithelial layer around atypical luminal cells of IC was preserved and positive for p63 and SMA, while the latter two antibodies were also positive in the spindle cells of branchioma (Fig. 5D). Cases 4 and 19 showed strong expression of AR in 60% and 100% of the tumor cells, respectively, mainly in the IC part (Fig. 5E).

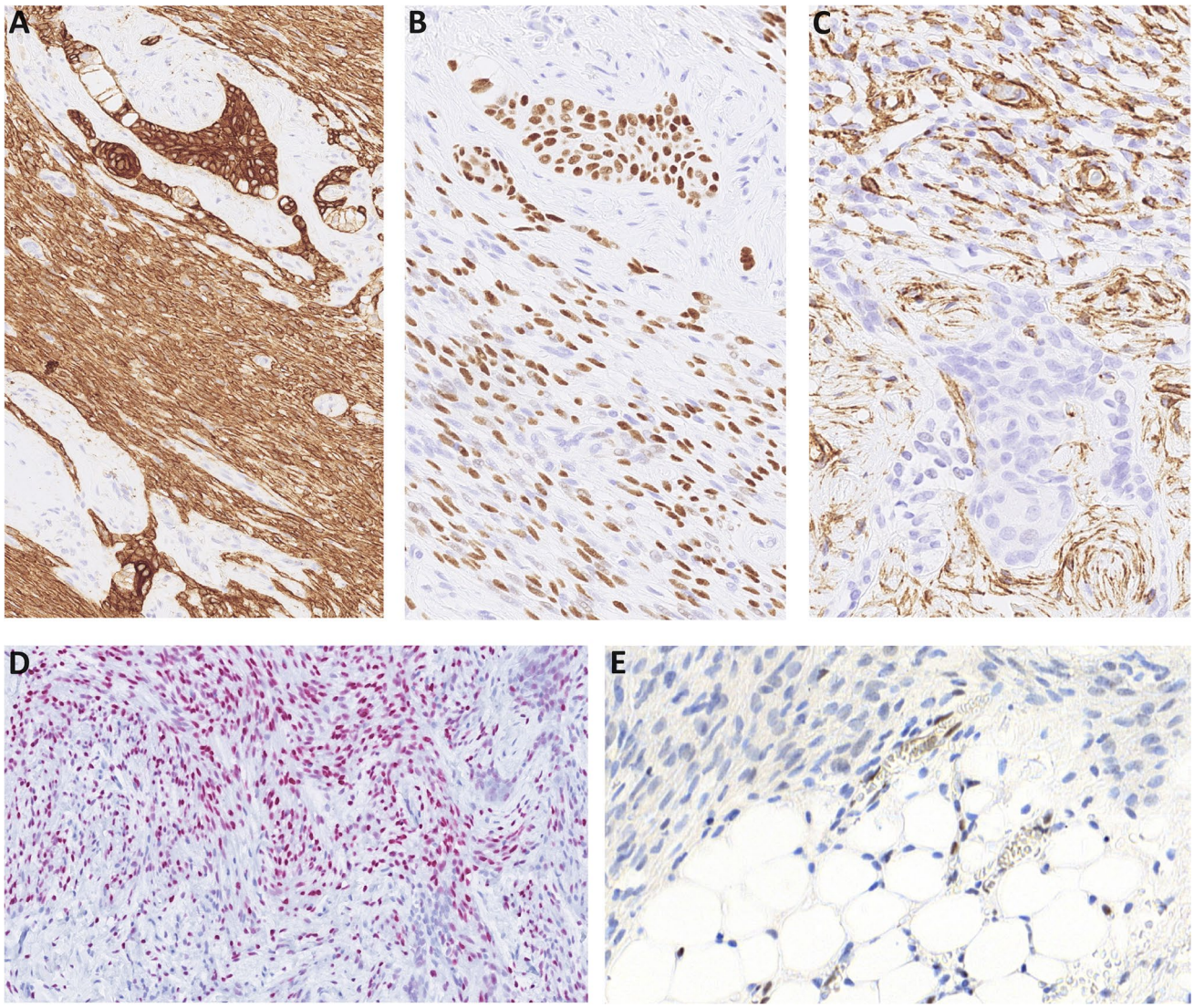

Fig. 4 Keratin cocktail AE1/3 (**A**) and p63 (**B**) were positive in both the epithelial and spindled cells. CD34 was positive in the spindle cells only (**C**). Androgen receptor was positive in most cases (**D**). Loss of tumor cell Rb1 expression (endothelial cells are a positive internal control) (**E**)

Case 13 was negative for AR. Rb1 was lost in all carcinoma cases (Fig. 5F). Proliferative activity was low, with a Ki-67 (MIB1) proliferation index was 1% in cases 4 and 13, reaching up to 15% in case 19.

Molecular testing

The results of targeted NGS and FISH are summarized in Table 5. Eight cases (8/23) had sufficient tissue and/or sufficient DNA quality for testing by NGS and/or FISH.

NGS testing was successful in six cases of classic branchiomas. In case 1, five pathogenic mutations were found, namely two different *MSH6* mutations, two different *PTEN* mutations, and *KRAS* mutation. In addition, two probably germline variants of unknown significance (VUS) in *ARID1A* and *PDGFRA* were detected. Case 2 showed only VUS including *BMPR1A* and *TET2* gene mutations. Case 14 showed a pathogenic *BRCA1* mutation. In case 20, a pathogenic mutation of *FANCG* gene and a VUS (probably germline mutation) of *NF1* gene were detected. Case 21 showed three VUS: *PHOX2B*, *XRCC2*, and *PLCG2*, the last two suspicious for germline origin. Finally, in case 22, NGS detected *NF2* and *NF1* gene mutations and two VUS including *NF1* and *PTCH1* genes. Tumor mutation burden was low.

In one case of carcinoma ex branchioma (case 19), we performed a microdissection of the IC component and branchioma component and we identified four pathogenic

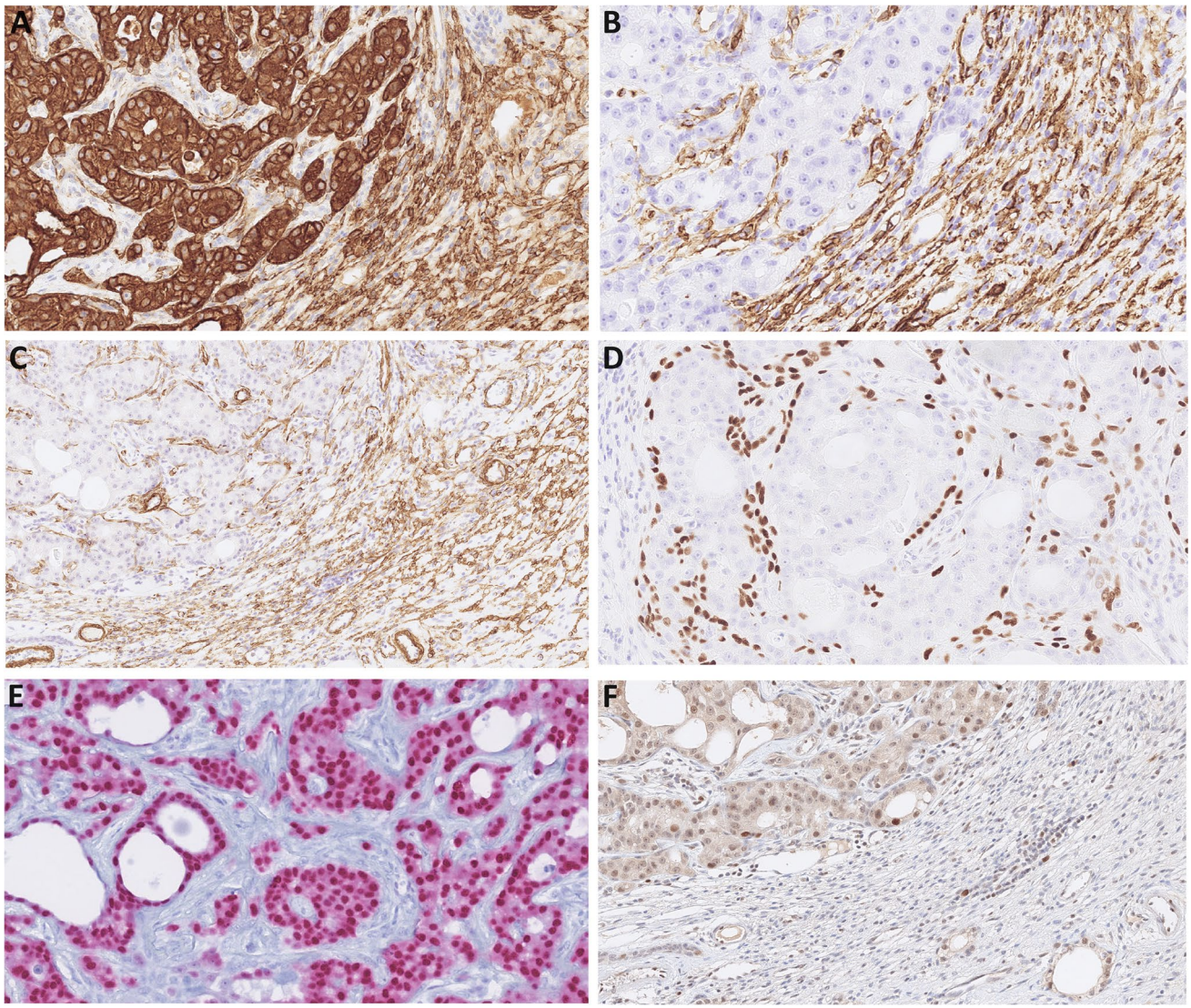

Fig. 5 Pancytokeratins were strongly immunoreactive in both carcinoma (left) and branchioma (right) components (**A**). CD34 decorated vascular structures in between carcinoma nests (left) and branchioma part (right) (**B**). An intact myoepithelial layer around atypical luminal cells was highlighted by SMA (**C**) and p63 (**D**). Androgen receptor was seen in 100% of cells of IC, while branchioma in the background was negative or showed only patchy and weak nuclear positivity (**E**). Rb1 immunoexpression was present only in scattered IC cells (< 5%) while the branchioma (right) was negative (lymphocytes are a positive internal control) (**F**)

mutations in IC including *HRAS*, *PIK3CA*, *CHD2*, and *SLIT2*, the latter was suspicious for germline mutation. In addition, six suspicious germline VUS were found, including *KMT2C*, *TET2*, *PIK3C2B*, *ABL2*, *FLT4*, and *PPARG* mutations. In the branchioma part, we found only the identical *SLIT2* mutation, and almost the same spectrum of VUS as in IC, while all other pathogenic mutations detected in the IC component were absent in the classical branchioma component.

In two cases (cases 14 and 18, both pure branchiomas), heterozygous deletion of *Rb1* was detected by FISH with loss in 92 and 88 nuclei of 100 counted, respectively.

Discussion

Branchiomas are very rare lower neck tumors with only four malignant cases described in the literature [2, 4–6, 17]. The molecular genetic background of branchiomas is still poorly understood, with only few manuscripts addressing this issue [6–8, 18]. In a letter to the editor, four branchiomas were evaluated using *PLAG1* FISH to rule out a possible relationship to pleomorphic adenomas [18]. No case from their study was positive for *PLAG1* rearrangements. In another molecular study, two cases of classic branchioma and one case of carcinoma ex branchioma (the latter case is included in the current study as case 19) were evaluated

Table 5 Molecular genetic with immunohistochemical correlation to Rb1 of selected cases

No	Age/sex		TruSight Oncology 500 NGS Kit (Illumina)		Copy number alteration		Rb1 IHC
			Pathogenic/likely pathogenic mutation	Variant of unknown clinical significance (VUS)	FISH Rb1 loss	FISH number of positive nuclei/100 cells	
1	78/M		*MSH6* c.3261dup p.(Phe1088LeufsTer5) AF: 18% MSH6 c.3202C > T p.(Arg1068Ter) AF: 23% *PTEN* c.385G > A p.(Gly129Arg) AF: 17% *PTEN* c.697C > T p.(Arg233Ter) AF: 9% *KRAS* c.437C > T p.(Ala146Val) AF: 8%	*ARID1A* c.4783A > G p.(Met1595Val) AF: 29% *PDGFRA* c.223G > C p.(Glu75Gln) AF: 45%*	Negative	32/100	Loss
2	43/M		Negative	*BMPR1A* c.776C > T p.(Ala259Val) AF: 6% *TET2* c.2429A > G p.(Gln810Arg) AF: 43%*	Negative	21/100	Loss
14	80/M		*BRCA1* c.160C > T p.(Gln54Ter) AF: 6%		**Positive**	**92/100**	Loss
18	51/M		Not analyzable		**Positive**	**88/100**	Loss
19	70/F	*IC*	***HRAS* c.181C > A p.(Gln61Lys) AF: 29%** ***PIK3CA* c.1624G > A p.(Glu542Lys) AF: 8%** *CHD2* c.4173dup p.(Gln1392ThrfsTer17) AF: 7% *SLIT2* c.162_163dup p.(Arg55ProfsTer9) AF: 40%*	*KMT2C* c.10403C > T p.(Pro3468Leu) AF: 47%* *TET2* c.434G > A p.(Ser145Asn) AF: 47%* *PIK3C2B c.3076G > A* p.(Val1026Met) AF: 48* *ABL2 c.3293G > A* p. (Ser1098Asn) AF: 52%* *FLT4 c.*4063G > A p. (Val1355Met) AF 48%* *PPARG c.147 T > G* p. (Asp49Glu) AF: 43%*	Negative	20/100	Loss in branchioma and 5% of positive cells in carcinoma
		B	*SLIT2 c.162_163dup p.(Arg55ProfsTer9) AF: 38%**	*PIK3C2B c.3076G > A* p.(Val1026Met) AF: 49%* *ABL2 c.3293G > A* p. (Ser1098Asn) AF: 51% * *FLT4 c.*4063G > A p. (Val1355Met) AF 47%* *PPARG c.147 T > G* p. (Asp49Glu) AF: 44%*			
20	50/M		*FANCG* c.1158del p.(Ser387ProfsTer16) AF: 5%	*NF1* c.7003A > G p.(Thr2335Ala) AF: 50%*	Negative	41/100	Loss
21	37/M		Negative	*PHOX2B* c.797C > T p.(Ala266Val) AF: 6% *XRCC2* c.662 T > C p.(Ile221Thr) AF: 48%* *PLCG2* c.406G > A p.(Ala136Thr) AF: 43%*	Negative	35/100	Loss
22	66/M		*NF2* c.1396C > T p.(Arg466Ter) AF: 36% *NF1* c.1765C > T p.(Gln589Ter) AF: 5%	*NF1* c.1802G > A p.(Arg601Gln) AF: 6% *PTCH1* c.28C > G p.(Pro10Ala)AF: 5%	Negative	24/100	Retained in the epithelial component but lost in the spindle cell component (< 10% of tumor cells)

*Suspicious germline mutation; *AF* allelic fraction, *B* branchioma, *FISH* fluorescence in situ hybridization, *IC* intraductal carcinoma, *IHC* immunohistochemistry, *M* male, *F* female

[6], with a pathogenic *HRAS* c.181C > A (p.Gln61Lys) mutation in the carcinoma component within the current study, two additional pathogenic mutations were identified: *PIK3CA* c.1624G > A p.(Glu542Lys) and *CHD2* c.4173dup p.(Gln1392ThrfsTer17). This case histologically, immunohistochemically, and genetically resembled salivary gland IC of apocrine subtype, in which the same *HRAS* and *PIK3CA* mutations have been reported [19, 20]. The final case report described adenocarcinoma arising from branchioma with *KRAS* and *TP53* gene mutations detected [7]. The adenocarcinoma histologically consisted of low-grade and high-grade components, and the authors suggested the potential responsibility of *KRAS* mutation for the development of adenocarcinoma and *TP53* alteration for the transition from low-grade to high-grade histology. The branchioma component did not contain any of the above-mentioned mutations [7].

The neuroendocrine-like branchioma (case 1) demonstrated five pathogenic mutations including *MSH6* mutations, two *PTEN* mutations, and one *KRAS* alteration [8]. Despite the presence of *MSH6* genetic alteration, MSH6 IHC was retained in tumor cells, which can be explained by unaltered antibody epitope for MSH6 in tumor cells with its positive nuclear expression. This study presents three additional cases of branchioma with identified pathogenic gene mutations, including case 14 with *BRCA1* c.160C > T p.(Gln54Ter), case 20 with *FANCG* c.1158del p.(Ser387ProfsTer16), and case 22 with *NF2* c.1396C > T p.(Arg466Ter) and *NF1* c.1765C > T p.(Gln589Ter). Despite the histological distinctness of branchiomas, the spectrum of altered genetic pathways is molecularly quite heterogeneous.

Two cases from our cohort showed *Rb1* gene heterozygous deletion by FISH. This finding, together with the neck location, loss of Rb1 immunoexpression, reactivity with CD34, and a spindle cell morphologic component, places branchiomas in a differential diagnosis with spindle cell predominant trichodiscoma and spindle cell lipoma [21–25]. An increasing number of tumor entities, originally thought to be completely indolent with no carcinogenic potential, are now being reclassified based on the finding of cancer-causing genetic mutations in a subset of them. The above discussed findings suggest that branchiomas might also represent such a precursor lesion, as carcinoma may occasionally develop within them. In this regard, they seem somewhat similar to IC ex sclerosing polycystic adenoma of salivary glands, which shares a similar molecular genetic features with alterations in the PI3K-AKT pathway as seen in one of the carcinoma ex branchioma cases [26–28].

When evaluating a lateral neck mass suspicious for branchioma, a spectrum of spindle cell neoplasms with cytokeratin immunoreactivity and potentially malignant behavior should be excluded. First, metastatic poorly differentiated SCC is at the forefront of the differential diagnosis. Poorly differentiated SCCs may develop a spindle cell phenotype, are often at least focally positive for pancytokeratin, p63/p40, and CK5/6, and are usually highly mitotically active. Furthermore, metastatic SCC from the oropharyngeal region may be p16 positive as a part of HPV-associated malignancies. However, in a subset of oropharyngeal SCC, Rb1 IHC loss has been reported and associated with better disease-free survival [29]. These tumors had retained p16 immunoexpression despite HPV negativity by RNA in situ hybridization. Synovial sarcoma (SS), biphasic or monophasic, is a relatively common mimic of branchioma, expressing pancytokeratin and showing both epithelial and spindle cell morphologies. SMA is positive in almost half of SS and CD34 may be present in a small subset of monophasic SS [30]. The panel of IHC markers used for further evaluation should include SS18-SSX/SS18 antibodies [31], which were not reported in branchiomas.

Another mimic is solitary fibrous tumor (SFT) which may display a variable fatty component (lipomatous subtype) and hence mimic branchioma [32]. SFT is also positive for CD34, but negative for various cytokeratin with a strong nuclear STAT6 expression by IHC and usually retained RB1 expression. Alternatively, *NAB2::STAT6* fusion can be demonstrated by molecular methods [33]. Recently, two groups have described mesenchymal-epithelial transdifferentation of SFT with well-developed epithelial cysts in the background of spindle cell proliferation and strong pancytokeratin immunoexpression [34, 35]. Thus, the demonstration of STAT6 alterations represents the most useful approach in diagnosing these tumors.

Herein, we performed the largest molecular genetic study of 23 cases of branchioma, with three cases of carcinoma arising within branchioma. These three cases had cribriform to solid morphology with histological resemblance to salivary IC of apocrine subtype. Five cases in our cohort showed molecular genetic alterations in different molecular genetic pathways. Eighteen cases showed loss of Rb1, and in two of these, there was a heterozygous deletion of *Rb1* gene. These findings broaden the spectrum of lateral neck lesions with Rb1 IHC loss and 13q/*Rb1* family of tumors.

Supplementary Information The online version contains supplementary material available at https://doi.org/10.1007/s00428-023-03697-1.

Author contribution MB, AA, MM, AS, and MM: conception and design of the work; acquisition, analysis, and interpretation of data; drafting the MS; and revising it critically for important intellectual content and scientific integrity. TV, PG, and VH performance and interpretation of molecular genetic analysis, revising it critically for important intellectual content and scientific integrity.

LDRT, MH, NR, DS, SL, NH, and RŽ: providing the case, reading and revising the MS critically for important intellectual content and scientific integrity.

All authors have read and approved the final manuscript.

Funding This study was in part supported by study grant SVV 260652 from the Ministry of Education, Czech Republic, the Cooperatio

Program, research area SURG, and the project National Institute for Cancer Research — NICR (Programme EXCELES, ID Project No. LX22NPO5102) — funded by the European Union-Next Generation EU.

Data availability All data generated or analyzed during this study are included in this published article.

Declarations

Ethics approval and consent to participate Sample was used in accordance with ethical guidelines. Informed consent was not required for the study.

Conflict of interest The authors declare no competing interests.

References

1. Jing H, Wang J, Wei H et al (2015) Ectopic hamartomatous thymoma: report of a case and review of literature. Int J Clin Exp Pathol 8:11776–11784
2. Michal M, Neubauer L (1993) Carcinoma arising in ectopic hamartomatous thymoma. A previously unpublished occurrence. Report of two cases. Zentralbl Pathol 139:381–386
3. Michal M, Zamecnik M, Gogora M et al (1996) Pitfalls in the diagnosis of ectopic hamartomatous thymoma. Histopathology 29:549–555
4. Michal M, Neubauer L, Fakan F (1996) Carcinoma arising in ectopic hamartomatous thymoma. An ultrastructural study. Pathol Res Pract. 192:610–618 (discussion 619-621)
5. Sato K, Thompson LDR, Miyai K et al (2018) Ectopic hamartomatous thymoma: a review of the literature with report of new cases and proposal of a new name: biphenotypic branchioma. Head Neck Pathol 12:202–209
6. Thompson LDR, Gagan J, Washington A et al (2020) Biphenotypic branchioma: a better name than ectopic hamartomatous thymoma for a neoplasm with HRAS mutation. Head Neck Pathol 14:884–888
7. Taniguchi N, Satou A, Ito T et al (2023) Adenocarcinoma arising in branchioma with a KRAS and TP53 mutation. Pathol Int 73(7):317–322
8. Baneckova M, Michal M, Vanecek T et al (2023) Branchioma with a nested/organoid morphology: molecular profiling of a distinctive potentially misleading variant and reappraisal of potential relationship to CD34-positive/Rb1-deficient tumors of the neck. Virchows Arch 483(4):541–548
9. Fetsch JF, Laskin WB, Michal M et al (2004) Ectopic hamartomatous thymoma: a clinicopathologic and immunohistochemical analysis of 21 cases with data supporting reclassification as a branchial anlage mixed tumor. Am J Surg Pathol 28:1360–1370
10. Kushida Y, Haba R, Kobayashi S et al (2006) Ectopic hamartomatous thymoma: a case report with immunohistochemical study and review of the literature. J Cutan Pathol 33:369–372
11. Weinreb I, O'Malley F, Ghazarian D (2007) Ectopic hamartomatous thymoma: a case demonstrating skin adnexal differentiation with positivity for epithelial membrane antigen, androgen receptors, and BRST-2 by immunohistochemistry. Hum Pathol 38:1092–1095
12. Michal M, Rubin BP, Kazakov DV et al (2020) Inflammatory leiomyosarcoma shows frequent co-expression of smooth and skeletal muscle markers supporting a primitive myogenic phenotype: a report of 9 cases with a proposal for reclassification as low-grade inflammatory myogenic tumor. Virchows Arch 477:219–230
13. Skalova A, Ptakova N, Santana T et al (2019) NCOA4-RET and TRIM27-RET are characteristic gene fusions in salivary intraductal carcinoma, including invasive and metastatic tumors: is "intraductal" correct? Am J Surg Pathol 43:1303–1313
14. Landrum MJ, Lee JM, Benson M et al (2018) ClinVar: improving access to variant interpretations and supporting evidence. Nucleic Acids Res 46:D1062–D1067
15. Michal M, Agaimy A, Contreras AL et al (2018) Dysplastic lipoma: a distinctive atypical lipomatous neoplasm with anisocytosis, focal nuclear atypia, p53 overexpression, and a lack of MDM2 gene amplification by FISH; a report of 66 cases demonstrating occasional multifocality and a rare association with retinoblastoma. Am J Surg Pathol 42:1530–1540
16. Michal M, Mukensnabl R (1999) Clear cell epithelial cords in an ectopic hamartomatous thymoma. Histopathology 35:89–90
17. Oh H, Kim E, Ahn B et al (2019) Adenocarcinoma arising in an ectopic hamartomatous thymoma with HER2 overexpression. J Pathol Transl Med 53:403–406
18. Liang PI, Li CF, Sato Y et al (2013) Ectopic hamartomatous thymoma is distinct from lipomatous pleomorphic adenoma in lacking PLAG1 aberration. Histopathology 62:518–522
19. Hsieh MS, Lee YH, Jin YT et al (2020) Clinicopathological study of intraductal carcinoma of the salivary gland, with emphasis on the apocrine type. Virchows Arch 477:581–592
20. Bishop JA, Gagan J, Krane JF et al (2020) Low-grade apocrine intraductal carcinoma: expanding the morphologic and molecular spectrum of an enigmatic salivary gland tumor. Head Neck Pathol 14:869–875
21. Michalova K, Kutzner H, Steiner P et al (2019) Spindle cell predominant trichodiscoma or spindle cell lipoma with adnexal induction? A study of 25 cases, revealing a subset of cases with RB1 heterozygous deletion in the spindle cell stroma. Am J Dermatopathol 41:637–643
22. Kutzner H, Kaddu S, Kanitakis J et al (2018) Spindle cell-predominant trichodiscoma. In: Elder DE, Massi D, Scolyer RA, Willemze R (eds) WHO classification of skin tumours, 4th en. IARC Press, Lyon, p 210
23. Dahlen A, Debiec-Rychter M, Pedeutour F et al (2003) Clustering of deletions on chromosome 13 in benign and low-malignant lipomatous tumors. Int J Cancer 103:616–623
24. Fletcher CD, Akerman M, Dal Cin P et al (1996) Correlation between clinicopathological features and karyotype in lipomatous tumors. A report of 178 cases from the Chromosomes and Morphology (CHAMP) Collaborative Study Group. Am J Pathol 148:623–630
25. Dal Cin P, Sciot R, Polito P et al (1997) Lesions of 13q may occur independently of deletion of 16q in spindle cell/pleomorphic lipomas. Histopathology 31:222–225
26. Bishop JA, Gagan J, Baumhoer D et al (2020) Sclerosing polycystic "adenosis" of salivary glands: a neoplasm characterized by PI3K pathway alterations more correctly named sclerosing polycystic adenoma. Head Neck Pathol 14:630–636
27. Hernandez-Prera JC, Saeed-Vafa D, Heidarian A et al (2022) Sclerosing polycystic adenoma: conclusive clinical and molecular evidence of its neoplastic nature. Head Neck Pathol 16:416–426
28. Skalova A, Baneckova M, Laco J et al (2022) Sclerosing polycystic adenoma of salivary glands: a novel neoplasm characterized by PI3K-AKT pathway alterations-new insights into a challenging entity. Am J Surg Pathol 46:268–280
29. Berdugo J, Rooper LM, Chiosea SI (2021) RB1, p16, and human papillomavirus in oropharyngeal squamous cell carcinoma. Head Neck Pathol 15:1109–1118
30. Pelmus M, Guillou L, Hostein I et al (2002) Monophasic fibrous and poorly differentiated synovial sarcoma: immunohistochemical reassessment of 60 t(X;18)(SYT-SSX)-positive cases. Am J Surg Pathol 26:1434–1440

31. Baranov E, McBride MJ, Bellizzi AM et al (2020) A novel SS18-SSX fusion-specific antibody for the diagnosis of synovial sarcoma. Am J Surg Pathol 44:922–933
32. Lee JC, Fletcher CD (2011) Malignant fat-forming solitary fibrous tumor (so-called "lipomatous hemangiopericytoma"): clinicopathologic analysis of 14 cases. Am J Surg Pathol 35:1177–1185
33. Barthelmess S, Geddert H, Boltze C et al (2014) Solitary fibrous tumors/hemangiopericytomas with different variants of the NAB2-STAT6 gene fusion are characterized by specific histomorphology and distinct clinicopathological features. Am J Pathol 184:1209–1218
34. Baneckova M, Michal M, Hajkova V et al (2022) Misleading morphologic and phenotypic features (transdifferentiation) in solitary fibrous tumor of the head and neck: report of 3 cases and review of the literature. Am J Surg Pathol 46:1084–1094
35. Stevens TM, Rooper LM, Bacchi CE et al (2022) Teratocarcinosarcoma-like and adamantinoma-like head and neck neoplasms harboring NAB2::STAT6: unusual variants of solitary fibrous tumor or novel tumor entities? Head Neck Pathol 16:746–754

The preliminary results of the study were presented as a poster presentation at the United States and Canadian Academy of Pathology's 112th Annual Meeting in Los Angeles, USA, March 11–16, 2023, New Orleans, Louisiana.